Image acquisition process simulator

Alix de Gouvello, Laurent Soulier, Antoine Dupret Cea

Image acquisition process simulator

Alix DE GOUVELLO, Laurent SOULIER, Antoine DUPRET

CEA, LIST - Nano-INNOV, Bât 862 - PC 172, F91191 Gif-sur-Yvette Cedex, France
alix.degouvello@cea.fr, laurent.soulier@cea.fr
antoine.dupret@cea.fr

Résumé – Pour concevoir un nouveau capteur, en particulier non conventionnel, explorer les options de mode d'acquisition avant sa réalisation permet de mesurer leur impact sur la qualité des images produites. Voire, cette exploration peut être faite en vue de l'optimisation d'un capteur pour une application. C'est pourquoi la maîtrise de la chaîne d'acquisition de l'image est un élément clef pour intégrer, dès la conception des capteurs, conventionnels ou non, les différents effets altérant l'image. Pour y répondre, un simulateur de chaîne d'acquisition d'images a été développé. La fidélité du simulateur aux phénomènes physiques impliqués (tels que la diffraction) et la prise en compte des bruits sont impératives pour obtenir des résultats représentatifs. Le simulateur a été conçu pour être très modulaire et prendre en compte des capteurs à types de fonctionnement variés mais aussi des capteurs hétérogènes - où différents modes d'acquisition peuvent être présents selon la position - de différentes surfaces, plusieurs bandes spectrales, divers temps d'intégration selon les pixels, différents ordres de lecture des pixels selon différentes formes de séquences temporelles. On peut également simuler des systèmes dont l'optique serait plus complexe, connaissant leur fonction de transfert optique. Chaque étape de simulation a été évaluée et le simulateur global a été testé sur des sources ponctuelles, des images simulées et réelles et des images aériennes haute définition.

Abstract – In order to design a new sensor, exploring acquisition mode options before manufacturing allows to measure their impact on the quality of resulting image and image processing. This exploration can even be done to optimize a sensor for a given application. Hence, from the very beginning of the design of conventional or unconventional sensors, mastering picture acquisition process is a keypoint to take into account every physical phenomenon that affects image quality. To achieve this goal, an image acquisition process simulator has been designed. In order to get accurate and reliable results, the simulator had to match physical phenomena (e.g. diffraction) and to model noises. The simulator has been designed to be as modular as possible to model pixels with various function modes - for instance a differentiated-by-zone acquisition mode -, different sizes, several spectral bands, several acquisition times, different reading orders. Our simulator can also model systems whose optical design is more complex, knowing their optical transfer function. Every step of the simulation has been evaluated and the simulator has been globally tested on point sources, simulated and real pictures and aerial high definition pictures.

Introduction

The aim is to model a given image acquisition system, as unconventional as it may be [7, 6, 3, 5] from the light reflected by a scene, through the optics and all the way to the photosensitive elements enabling photoconversion and to the analog to digital converter. The challenge is to be physically realistic, while being fast, modular and keeping the model as simple as possible, to test the impact of the acquisition system on a given application or the image quality. To the best of our knowledge, no existing open source simulator is able to meet these expectations. Multi-physical simulators are incomplete, or too complex and thus too difficult to use to test a large range of configurations. In a first section, we will give an overview of the different steps our modeling involves. Then, the physical phenomena involved and the simulated photo-conversion are explained respectively in section 2 and 3. In section 4, we present the tests that were made to assert the quality of the simulator given different entry settings.

1 Model overview

We chose to model the scene to image by an irradiance matrix that is deduced for each given wavelength band from a high definition deconvoluted image which will serve as ground truth, the maximal irradiance of the scene and the mean irradiance, through a linear modeling of irradiance values. Then the optical system is either modeled by its optical transfer function (OTF) or a "simple" OTF is deduced from the physical description of the optics. The geometrical parameters of the system are also needed. Diffraction and vignetting are thus taken into account. Discretization of the source image, the pupil and the image plane of the sensor implies some model limitations that will be described later and also a normalization factor for the energy to be conserved. The whole process is described on Figure 1.

2 Radiometry and electromagnetism details

The entry signal is an irradiance matrix. Irradiance is the energy emitted by a given surface, in a given solid angle by unit of time, for a given wavelength (in $\mathrm{W.m^{-2}.sr^{-1}.\lambda^{-1}}$). Lacking further information about the scene, we assume that the Bidirectional Reflectance Distribution Function (BDRF) of the objects is merged into the source image and that it does not

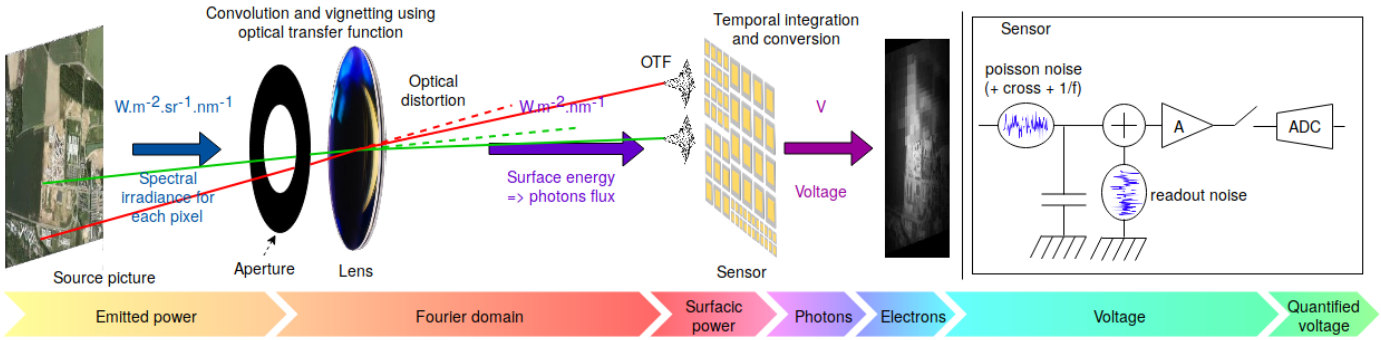

FIGURE 1 – Model overview

modify diffraction modeling.

2.1 Optical system

Each pixel of the source image is considered as a point source emitting a spherical wave. Its energy is scattered over half a sphere. Its magnitude decreases from the source to a point of the space as the inverse of the distance. Here is a scheme to explain our notations :

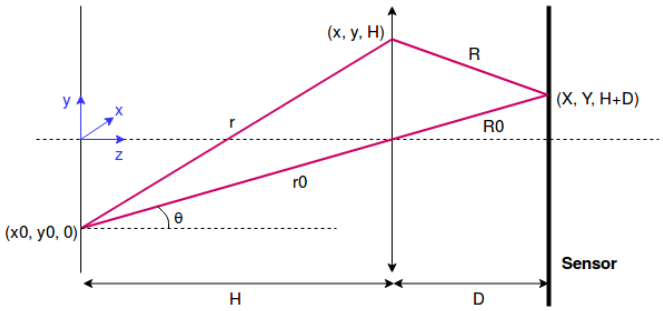

FIGURE 2 – The notations used in our calculations

Besides, let p_0 be the size of a pixel of the initial irradiance matrix, $\mathcal{A}_0$ the amplitude of the wave stemming from source pixel located at $(x_0, y_0, 0)$ and λ its wavelength, T the transmission function of the pupil and $\mathcal{FT}$ be the Fourier transform. Then, taking into account diffraction [1] and vignetting and considering the lens as a phase shifter, the amplitude of the wave at point $(X, Y, H + D)$ of the image plane is given by equation 1.

$$\mathcal{A}(X,Y) = \frac{\mathcal{A}_0 p_0}{H\lambda R_0}\sqrt{\frac{\cos^3(\theta)}{2\pi}} \mathcal{FT}\{T(x,y)\}\left(\frac{x_0}{\lambda r_0} - \frac{X}{\lambda R_0}, \frac{y_0}{\lambda r_0} - \frac{Y}{\lambda R_0}\right) \quad (1)$$

The Fourier transform derives from the diffraction. The $\cos^3(\theta)$ term accounts for vignetting and it is a simple geometrical term. The other factors are due to change of variables or energy conservation : the energy that goes through the pupil is the same as the energy received by the sensor. The Fraunhofer diffraction is considered and the modeling is valid if D is close to the focal length of the lens located in the aperture and "large enough" with respect to sensor size.

Then, for full image modeling, we suppose that the light source is not coherent as it is mainly the case with natural scenes under natural light illumination. Thus, on the sensor surface, we consider the summation of energy instead of the complex phase amplitude summation.

As for the optical distortion, the major hypothesis is to assume that distortion and optical transfer function can be decoupled so that distortion can be implemented as a module separate from the rest of the optics.

2.2 Photo-noise

Due to the quantized nature of light, photon detection is a probabilistic phenomenon described by a Poisson distribution that is well approximated by a normal distribution. That is what is implemented in the simulator, the standard deviation being the number of photons expected to be detected at a given photo site.

3 Photo-conversion

Photo-conversion is described in several books such as, for instance, [2]. The process is described on the right of Figure 1. The quantum efficiency of a sensor depends, among other parameters, on the wavelength, on the material that is used, and, in case of a semiconductor, on how it is doped, the geometries and voltages. Thus no simple generic mathematical expression can be derived. Hence, the spectral quantum efficiency is approximated by an interpolation function of tabulated values.
In this paper, we present results of simulations for which the integration mode is the one chosen. Hence, the conversion from electrons to voltage is equivalent to the discharge of a capacitor later amplified and than quantized on N bits.

Readout noise is modeled by a gaussian distribution and electronic cross talk is seen as a convolution of the number of electrons in each photo site by a given diffusion matrix but is more thoroughly described in [4] . Results are tested by computing Signal to Noise Ratio (SNR) for a large range of values and verifying the slope of the evolution of the SNR plotted against

the signal value. As can be seen on Figure 3, the shape of the curve is in agreement with usual SNR evolution and with the model that predicts that readout noise is predominant for the small values whereas it is photo noise for higher irradiances [8].

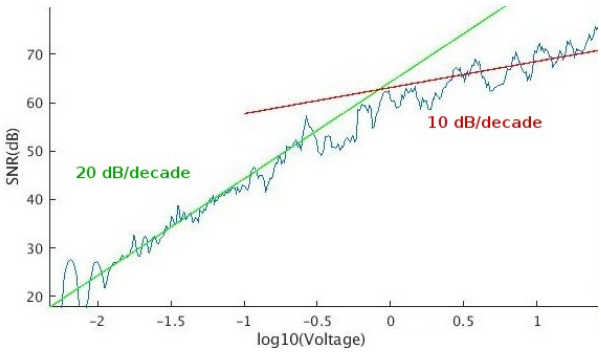

FIGURE 3 – Signal to Noise Ratio (dB) against decimal logarithm of exit voltage (V)

4 Numerical implementation

4.1 Discretization

Numerical simulation implies a discretization of the energy in the image plane, which in turn implies a discretization of the pupil. For the sake of simplicity, the same sampling as for the source image is chosen. Let (M, N) be the dimensions (in pixels) of the irradiance source matrix that is indexed by (n, m). So, after discretization, summing on all source pixels, we get the energy $\mathcal{E}$ received by one pixel (p, q) of the image plane (equation 2).

$$\mathcal{E}(p,q) = \frac{\lambda^2 H^2}{2\pi R_0^2 N^2 M^2 p_0^2} \mathcal{DFT}^{-1}(\mathcal{DFT}(|\mathcal{A}_0|^2 cos^3(\theta)) \mathcal{DFT}(|\mathcal{DFT}\{Q(n,m)\}|^2)) \quad (2)$$

With $Q(n,m) = T\left(\frac{n\lambda H}{Np_0}, \frac{m\lambda H}{mp_0}\right)$. Then this energy is converted into a number of photons received by each photo site, the energy of one photon is $E_{photon} = hc/\lambda$ with h the Planck's constant, c the speed of light and λ the wavelength. So the calculation is done for each wavelength, as is the photo conversion.

Then, the energy is integrated on rectangular surfaces corresponding to the pixels defined by the sensor architecture.

Sometimes, the discretization of the pupil implied by the discretization of the image plane is too coarse. This problem could be solved by oversampling the image plane to get a finer sampling step of the pupil.

4.2 Implementation

As has already been said, the simulator has been designed to be highly modular. It was first developped using MATLAB but will be ported to C++. Any optical system can be modeled by its Optical Transfer Function (OTF) that is why provided this OTF is known, for instance from a multi-physical simulator, the acquisition of images through any optical system can be simulated. Moreover, classical matrices of homogeneous pixels can be defined but our system also handles unconventional pixels organizations defined by a list of pixels locations and shapes on the sensor surface. If we want to have various acquisition timing, we can define several lists of pixels with one frequency by list and also simulate several acquisition times for different types of pixels.

5 Simulation tests

5.1 Classical sensor

Our first global test was to simulate the acquisition of a single elementary light source for a single wavelength, without any noise, by a classical sensor given a set of geometrical conditions that would enable the diffraction to be perceived to make sure we got an Airy disk and correctly simulated diffraction (see Figure 4).

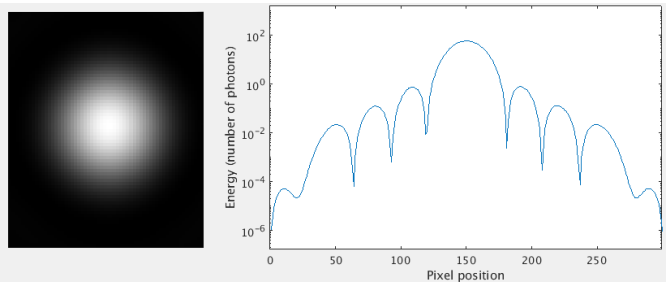

FIGURE 4 – Simulated Airy disk and cross-section of energy (y-log scale)

5.2 Non-conventional sensor

FIGURE 5 – Source aerial picture [Source : Géoportail]

To test for unconventional sensor, we took an aerial high definition picture and defined a list of pixels with 4 different zones of pixel sizes. Here are the source RGB picture (Figure 5) and the result we get for one of the 3 channels (Figure 6). Pixel sizes are expressed in arbitrary units because what matters here is the (focal length, pixel size) pair. Sizes of the pixels are cho-

sen to be visually meaningful, not to simulate a specific existing sensor.

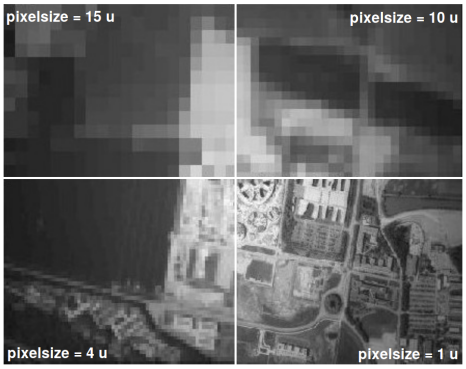

FIGURE 6 – Result picture of unconventional 4 zones sensor acquisition

5.3 Test for distortion

Finally we test distortion model realism, the Brown-Conrady distortion model is implemented with 2 radial distortion coefficients and 2 tangential distortion parameters. Distortion parameters need to be determined through calibration. The test is explained on the following scheme :

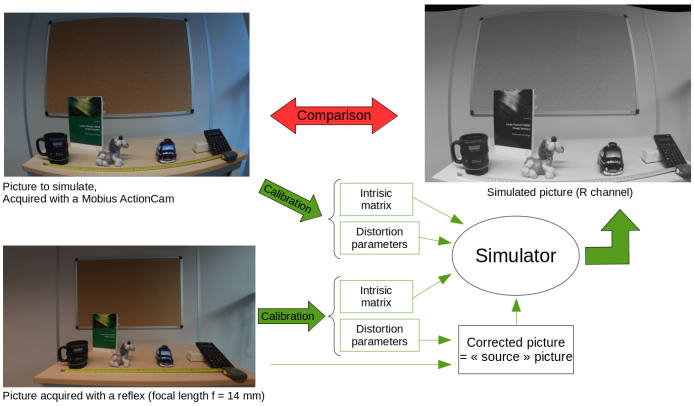

FIGURE 7 – Distortion test scheme

The result seems qualitatively visually acceptable, except on the edges where we reach the limits of the model. Other distortion models could be tested in future works, especially for wide-angle cameras.

Conclusion and perspectives

In this work we report the development of a versatile simulator for vision sensor system. Its purpose is to be used to test different design parameters combinations when working on new sensors but also for co-design of a vision-based application and a sensor.

The simulator features a realistic modeling of physical phenomena from electromagnetism to electronic conversion. At each step of the flow, the simulator has been evaluated to check its agreements to physics. The simulator has been tested on various representative pictures : simulated sources, test patterns and real pictures. The simulations appear to match ground truth qualitatively and with respect to low level metrics such as SNR profiles.

The implementation has been designed to be as modular as possible, in order to handle not only simple, conventional, synchronous systems but also more exotic ones. The architecture of the simulator thus makes it possible to define different pixel sizes and various integration times (e.g. for the different pixels within a single sensor) and unconventional pixels organizations (not only regular arrays of pixels). With its close connection to physics, the simulator enables various wavelengths to be taken into account and to define several acquisition spectral bands. Several reading orders of the pixels can be considered : snapshot and rolling shutter but also more original reading orders. Eventually, pixels characteristics can be the same for the whole sensor but they can also be defined on a per pixel basis.

The modularity of our simulator design makes several enhancements imaginable such as refining the model for small apertures. Future works will include using this simulator for co-designing innovative sensors.

References

[1] E. Aristidi. Diffraction. `http://sites.unice.fr/site/aristidi/optique/`.

[2] S. U. Ay. *Large Format CMOS Image Sensors : Performance and Design*. VDM, Verlag Dr. Müller, 2008.

[3] T. Delbrück, B. Linares-Barranco, E. Culurciello, and C. Posch. Activity-driven, event-based vision sensors. In *Circuits and Systems (ISCAS), Proceedings of 2010 IEEE International Symposium on*. IEEE, 2010.

[4] I. Djite, M. Estribeau, P. Magnan, G. Rolland, S. Petit, and O. Saint-Pe. Theoretical models of modulation transfer function, quantum efficiency, and crosstalk for CCD and CMOS image sensors. *IEEE Transactions on Electron Devices*, 2012.

[5] L. Millet et al. A 5500-frames/s 85-GOPS/W 3-D stacked BSI vision chip based on parallel in-focal-plane acquisition and processing. *IEEE Journal of Solid-State Circuits*, 2019.

[6] R. Serrano-Gotarredona et al. CAVIAR : A 45k neuron, 5M synapse, 12G connects/s AER hardware sensory–processing–learning–actuating system for high-speed visual object recognition and tracking. *IEEE Transactions on Neural Networks*, 2009.

[7] S. Xia, R. Sridhar, P. Scott, and C. Bandera. An all CMOS foveal image sensor chip. pages 409 – 413, 10 1998.

[8] D. XD Yang and A. El Gamal. Comparative analysis of snr for image sensors with enhanced dynamic range. In *Sensors, Cameras, and Systems for Scientific/Industrial Applications*, volume 3649, pages 197–212. International Society for Optics and Photonics, 1999.